2016

Class-switched anti-insulin antibodies originate from unconventional antigen presentation in multiple lymphoid sites

Xiaoxiao Wan
Washington University School of Medicine in St. Louis

James W. Thomas
Vanderbilt University Medical School

Emil R. Unanue
Washington University School of Medicine in St. Louis

Class-switched anti-insulin antibodies originate from unconventional antigen presentation in multiple lymphoid sites

Xiaoxiao Wan,[1] James W. Thomas,[2] and Emil R. Unanue[1]

[1]Department of Pathology and Immunology, Washington University School of Medicine, St. Louis, MO 63110
[2]Department of Medicine, Vanderbilt University Medical School, Nashville, TN 37232

Autoantibodies to insulin are a harbinger of autoimmunity in type 1 diabetes in humans and in non-obese diabetic mice. To understand the genesis of these autoantibodies, we investigated the interactions of insulin-specific T and B lymphocytes using T cell and B cell receptor transgenic mice. We found spontaneous anti-insulin germinal center (GC) formation throughout lymphoid tissues with GC B cells binding insulin. Moreover, because of the nature of the insulin epitope recognized by the T cells, it was evident that GC B cells presented a broader repertoire of insulin epitopes. Such broader recognition was reproduced by activating naive B cells ex vivo with a combination of CD40 ligand and interleukin 4. Thus, insulin immunoreactivity extends beyond the pancreatic lymph node–islets of Langerhans axis and indicates that circulating insulin, despite its very low levels, can have an influence on diabetogenesis.

In humans and non-obese diabetic (NOD) mice, insulin autoreactivity is a prominent feature during the initiation and progression of type 1 diabetes (T1D; Nakayama et al., 2005; Zhang et al., 2008; Mohan et al., 2010; Unanue, 2014). Insulin autoantibodies (IAAs) are used as important predictive biomarkers for disease susceptibility and prognosis (Zhang and Eisenbarth, 2011). Although IAAs can be of the IgM or IgG class (Bodansky et al., 1986; Dean et al., 1986), IgG IAAs are associated with robust diabetes progression (Achenbach et al., 2004; Hoppu et al., 2004). These findings point to an essential role of CD4 T helper cells in supporting generation of class-switched IAAs through cognate interactions with anti-insulin B cells. However, issues concerning the source of T cell help, the nature of the T cell–B cell interaction, and the sites of IAA production remain largely unexplained.

In this study, we have examined the interactions between insulin-reactive T and B cells in NOD mice with a goal of identifying the nature and sites of T cell–B cell interactions and their consequences. We previously identified CD4 T cells to insulin that escaped thymic negative selection, entered islets of Langerhans, and caused diabetes, of which the 8F10 T cell, used here as a TCR transgenic mouse, is representative (Mohan et al., 2013). The 8F10 mice had IAAs in relatively high titers directed to conformational insulin, but these T cells specifically recognize the 12–20 sequence of the insulin B chain (B:12-20), an epitope that is not presented from the processing of insulin (Mohan et al., 2011, 2013). Insulin processing by APCs, including B cells, generates a close but distinct sequence; that is, from 13–21 (B:13-21), a one–amino acid shift in the MHC-binding register (Mohan et al., 2011). However, the B:12-20 epitope is presented in islets from secretory granules containing catabolites of insulin that are transferred to intra-islet resident APCs (Mohan et al., 2010; Vomund et al., 2015). Studying this CD4 T cell is important for two reasons. First, because a majority of the insulin-reactive T cells recognize the B:12-20 epitope (Mohan et al., 2010, 2011), it remains to be defined how this T cell can interact with anti-insulin B cells and support IAA production when B cells that take up insulin should not present it. Second, it considers where the interaction is taking place; that is, whether insulin presentation is restricted to the pancreatic LNs (pLNs) or extended to other peripheral sites. The present view is that the pLN that drains the islets is a key site for the autoimmune process to move forward (Höglund et al., 1999; Gagnerault et al., 2002; Levisetti et al., 2004). Insulin circulates at low picomolar levels, an amount that is most likely below a threshold for effective T cell–B cell interactions outside the islet–pLN axis. But, notably, endogenous insulin has been shown to have an effect in modulating immature anti-insulin B cells in the bone marrow (Henry et al., 2009; Henry-Bonami et al., 2013) and mature B cells in the spleen (Rojas et al., 2001; Acevedo-Suárez et al., 2005).

Examining anti-insulin T cell–B cell interaction is hindered by the difficulty of tracking the insulin specificity in the polyclonal BCR repertoire. This limitation can be overcome by the V_H125.NOD anti-insulin BCR heavy chain transgenic model developed by one of us (Rojas et al., 2001). The V_H125 BCR heavy chain pairs with various endogenous light chains, giving rise to 1–3% insulin-specific B cells of the

Correspondence to Emil R. Unanue: unanue@wustl.edu

Abbreviations used: aLN, axillary LN; GC, germinal center; HEL, hen egg lysozyme; IAA, insulin autoantibody; iLN, inguinal LN; mLN, mesenteric LN; NOD, non-obese diabetic; pLN, pancreatic LN; T1D, type 1 diabetes.

The Rockefeller University Press $30.00
J. Exp. Med. 2016 Vol. 213 No. 6 967–978
www.jem.org/cgi/doi/10.1084/jem.20151869

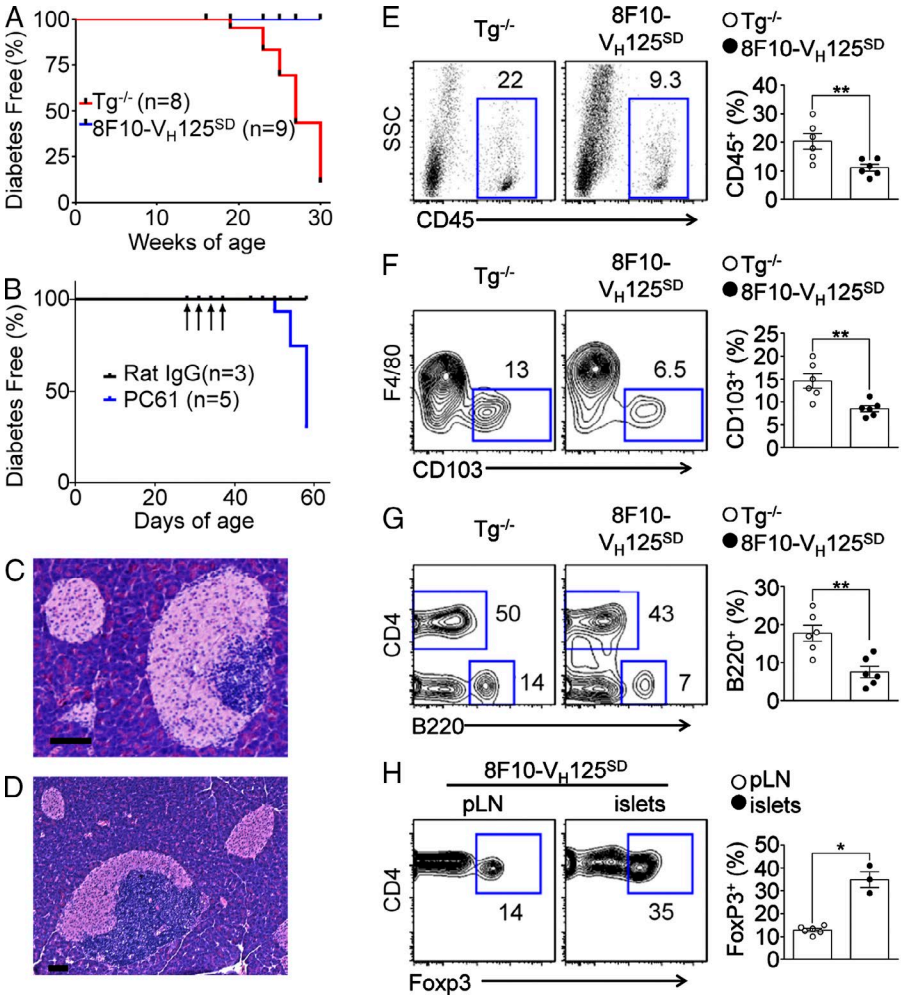

Figure 1. **Diabetes development and islet infiltration in the 8F10-V_H125^{SD} mice.** (A) Percentage of diabetes-free age-matched female mice in nontransgenic ($Tg^{-/-}$) and 8F10-V_H125^{SD} strains. (B) Percentage of diabetes-free 8F10-V_H125^{SD} mice given anti-CD25 (PC61) antibody or control rat IgG treatment. The arrows indicate the time point of antibody administration. (C–H) Islets from 8-wk-old female nontransgenic and 8F10-V_H125^{SD} mice were analyzed. (C) Hematoxylin and eosin staining of pancreatic sections from the 8F10-V_H125^{SD} mice showing representative healthy and peri-insulitic islets. (D) Hematoxylin and eosin staining of pancreatic sections from 8F10-V_H125^{SD} mice showing healthy and mild intra-insulitic islets. Bars, 50 µM. (E) FACS plots (left) and quantification (right) showing the frequency of the $CD45^+$ leukocytes among total islet cells (gated on live and singlets). (F) FACS plots (left) and quantification (right) showing the frequency of the $CD103^+$ DCs in $CD45^+CD11c^+$ gated islet cells. (G) FACS plots (left) and quantification (right) showing the frequency of the $CD4^+$ and $B220^+$ cells in $CD45^+$ gated islet cells. (H) FACS plots (left) and quantification (right) showing the frequency of the $FoxP3^+$ cells among $CD45^+CD4^+CD8^-$ T cells in the pLN and islets of the 8F10-V_H125^{SD} mice. *, $P < 0.05$; **, $P < 0.005$; Mann-Whitney test. Each point in E–H represents results of individual mice obtained from three independent experiments (mean ± SEM).

repertoire (Hulbert et al., 2001; Henry-Bonami et al., 2013). A recent study directly targeted the rearranged V_H125 variable region genes into the endogenous IgH locus (Williams et al., 2015). Consequently, the anti-insulin B cells formed in the resulting V_H125^{SD} mice are capable of class-switch recombination, permitting assessment of the IgG class of IAAs.

In this study, the 8F10 and V_H125^{SD} mouse strains were crossed and examined. The 8F10 T cells provided help to anti-insulin B cells, leading to germinal center (GC) formation and IAA production. The T cell–B cell interaction took place because activated GC B cells acquired altered insulin processing, resulting in presentation of the B:12-20 epitope to 8F10 T cells. Furthermore, insulin-specific GC formation was observed in multiple LNs and spleens, most likely resulting from the low level of insulin in the blood or lymph.

RESULTS

Two approaches to study the interactions between insulin-specific CD4 T cells and B cells

Insulin-specific T cell–B cell interactions were examined in two complementary models. In one, we crossed 8F10 TCR transgenic mice with the V_H125^{SD}.NOD BCR transgenic mice. In this model, the pathogenicity of 8F10 T cells was suppressed by strong regulatory mechanisms that prevented spontaneous diabetes. Our previous study showed that the 8F10 mice developed diabetes only when crossed onto the $Rag1^{-/-}$ background that excludes TCR α-chain rearrangement and T regulatory cell (T reg cell) development (Mohan et al., 2013). As shown in Fig. 1 A, none of the female 8F10-V_H125^{SD} mice developed diabetes, whereas the nontransgenic ($Tg^{-/-}$) littermates did. Indeed, experiments in progress indicate that treatment of these mice with anti-CD25 (PC61) antibody resulted in diabetes development in three out of five mice, whereas no mice under the isotype control antibody treatment became diabetic (Fig. 1 B).

At 8 wk of age, the islets of the 8F10-V_H125^{SD} mice displayed a heterogeneous profile of inflammation, as manifested by coexistence of peri-insulitic and mild intra-insulitic lesions (Fig. 1, C and D). Flow cytometry analyses revealed a significantly lower frequency of $CD45^+$ leukocytes infiltrating the islets of 8F10-V_H125^{SD} mice relative to $Tg^{-/-}$ littermates (Fig. 1 E). Furthermore, infiltration of $CD103^+$ DCs, a

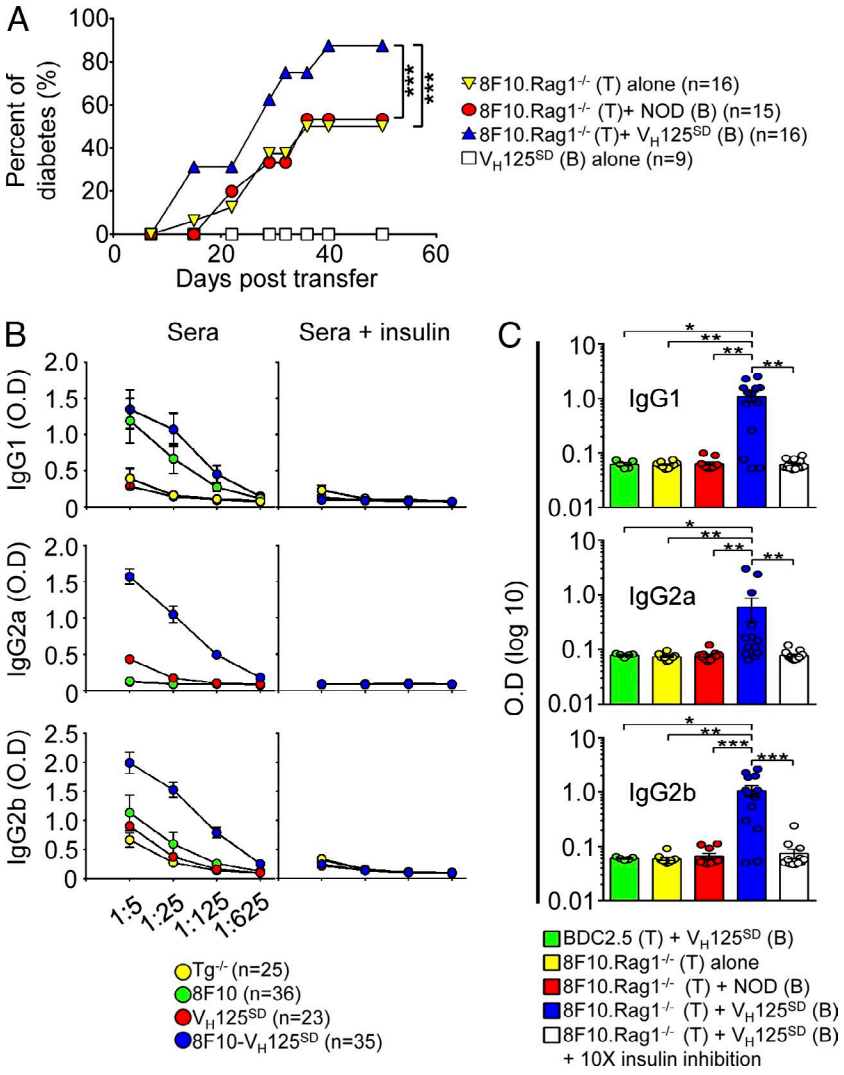

Figure 2. **Anti-insulin T cell–B cell interaction exacerbates diabetes transfer and leads to production of IAAs.** (A) Incidence of diabetes in NOD.Rag1$^{-/-}$ recipients given the indicated combinations of T and/or B cells. FACS-sorted naive T cells ($CD4^+CD8^-B220^-CD25^-CD62L^{hi}CD44^-$) from 8F10.Rag1$^{-/-}$ mice were transferred with or without B cells ($CD19^+CD4^-CD8^-IgMa^+GL7^-IgG^-$) sorted from V_H125^{SD} or WT NOD mice. ***, $P < 0.0005$; log-rank test. (B) Titers and specificity of IAAs in 8F10-V_H125^{SD} double transgenic mice. Sera collected from 4–9-wk-old 8F10-V_H125^{SD} mice were pooled, serially diluted, and examined by ELISA. Sera from age-matched littermates, including nontransgenic (Tg$^{-/-}$), 8F10, and V_H125^{SD} single transgenic mice, were also examined. To determine the specificity of IAAs, one aliquot of sera was incubated with a 10-fold excess of insulin (right) before measurement. (C) ELISA assays in sera of NOD.Rag1$^{-/-}$ recipients given indicated combinations of T and/or B cells sorted as in A. FACS-sorted naive BDC2.5 T cells ($CD4^+CD8^-B220^-CD25^-CD62L^{hi}CD44^-$) were transferred as controls. The sera were collected on day 30 after transfer, and each symbol represents an individual mouse. *, $P < 0.05$; **, $P < 0.005$; ***, $P < 0.001$; Mann-Whitney test. Data represent cumulative results (mean ± SEM) from at least three independent experiments.

process required for diabetes development (Ferris et al., 2014), was also limited in the double transgenic mice (Fig. 1 F). Infiltration by the $B220^+$ B cells was significantly less in the 8F10-V_H125^{SD} than the Tg$^{-/-}$ littermates (Fig. 1 G). $FoxP3^+$ T reg cells were found in the pLN, and more strikingly, a significantly higher number of $CD4^+$ T cells in the islets of the 8F10-V_H125^{SD} mice were FoxP3 positive (Fig. 1 H).

The second model consisted of transferring naive T cells ($CD4^+CD8^-B220^-CD25^-CD62L^{hi}CD44^-$) isolated from 8F10.Rag1$^{-/-}$ mice and B cells ($CD19^+CD4^-CD8^-IgMa^+GL7^-IgG^-$) from the V_H125^{SD} mice into NOD.Rag1$^{-/-}$ recipients. Under this approach, diabetes developed. Transfer of V_H125^{SD} B cells did not induce diabetes during a 50-d monitoring period (Fig. 2 A). Transfer of 8F10.Rag1$^{-/-}$ T cells alone or together with B cells from conventional NOD mice induced diabetes with a similar kinetics (Fig. 2 A). Conventional NOD B cells did not exacerbate diabetes transfer, possibly because of a low number of anti-insulin B cells in the repertoire. Indeed, B cells from the V_H125^{SD} mice significantly enhanced the ability of 8F10.Rag1$^{-/-}$ T cells to drive diabetes (Fig. 2 A). These results indicate the importance of anti-insulin T cell–B cell cooperation in promoting diabetes development, in agreement with previous studies showing the capacity of the V_H125 BCR in exacerbating diabetes (Hulbert et al., 2001).

IAA production in the two models

The sera of the 8F10-V_H125^{SD} mice contained the highest titers of IAAs across the IgG1, IgG2a, and IgG2b subclasses relative to the 8F10,V_H125^{SD}, and Tg$^{-/-}$ littermates (Fig. 2 B, left). Low levels of IAAs with each IgG subclass were found in the Tg$^{-/-}$ and V_H125^{SD} mice (Fig. 2 B, left). Most of the IAAs in the 8F10 mice were IgG1, with some moderate levels of IgG2b (Fig. 2 B, left). Importantly, the IAAs were blocked by excess free insulin, indicating their specificity to conformational insulin (Fig. 2 B, right). Antibodies to denatured insulin or free 9–23 peptide were not detected (not depicted). Thus, 8F10 T cells promote production of class-switched IAAs recognizing native insulin.

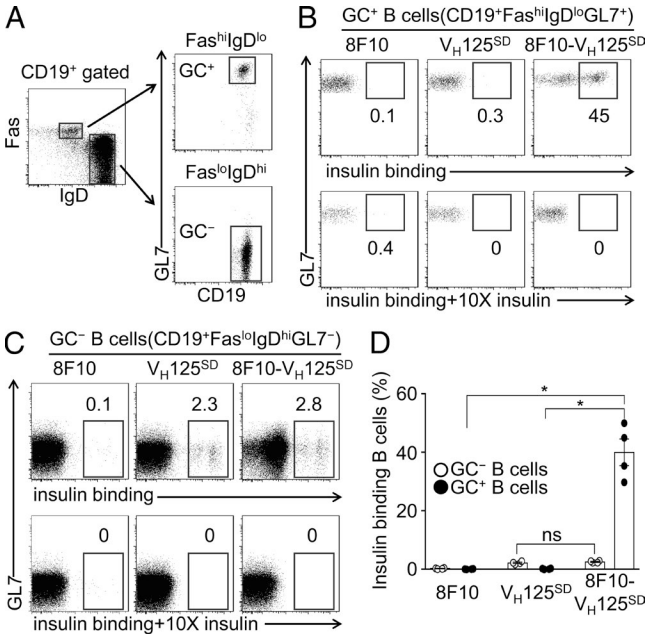

Figure 3. **8F10 T cell help is essential for GC differentiation of anti-insulin B cells.** (A) Gating strategy of GC^+ and GC^- B cells. (B and C) Insulin binding of the GC^+ (B) and GC^- (C) B cells from the pLNs of the 8F10, V_H125^{SD}, and 8F10-V_H125^{SD} mice. The insulin-binding B cells were identified by staining with biotinylated insulin followed by fluorochrome-conjugated streptavidin (top), and the specificity of insulin binding was determined by adding 10× insulin (bottom). (D) Quantification of the frequency of insulin-binding B cells among the GC^- or GC^+ B cells (mean ± SEM) as assessed in B and C. *, $P < 0.05$; Mann-Whitney test. Data in A–C are representative of four independent experiments, and each symbol in D represents one individual experiment.

In the second model of NOD.$Rag1^{-/-}$ mice transferred with 8F10.$Rag1^{-/-}$ T cells plus V_H125^{SD} B cells, diabetes developed with concomitant IAA production encompassing IgG1, IgG2a, and IgG2b subclasses (Fig. 2 C). These mice had significantly higher titers of IAAs than NOD.$Rag1^{-/-}$ recipients of 8F10.$Rag1^{-/-}$ T cells alone or 8F10.$Rag1^{-/-}$ T cells plus WT B cells (Fig. 2 C). The IAAs specifically recognized native insulin as indicated by their inhibition with free insulin (Fig. 2 C). Of note, the non–insulin-reactive BDC2.5 T cells, when cotransferred with V_H125^{SD} B cells, did not induce IAA production (Fig. 2 C). Thus, in the T cell–B cell cotransfer model, IAAs originate from specific anti-insulin T cell–B cell interactions that promote diabetes progression.

GC B cells in the presence of 8F10 T cells

The high titer of class-switched IAAs in the 8F10-V_H125^{SD} mice indicates active insulin-specific GC responses. We examined the B cells from the pLN for their reactivity to insulin by flow cytometry. The GC (GC^+) B cells were defined as $CD19^+Fas^{hi}IgD^{lo}GL7^+$ and the non-GC (GC^-) B cells as $CD19^+Fas^{lo}IgD^{hi}GL7^-$ (Fig. 3 A). Insulin-specific B cells were identified by their binding to biotinylated insulin in the presence or absence of a 10-fold excess of unlabeled insulin.

Strikingly, 45% of the GC^+ B cells in the pLNs of the 8F10-V_H125^{SD} mice bound insulin, and the binding was completely blocked by excess soluble insulin (Fig. 3 B, right). The non-GC insulin-binding B cells were few in the 8F10-V_H125^{SD} (2.8%) mice, consisting of two sets distinguished by the mean fluorescence intensities of the biotinylated insulin staining (Fig. 3 C, top). This is likely because the V_H125^{SD} BCR heavy chain pairs randomly with endogenous light chains, giving rise to BCRs with different affinities to insulin (Henry et al., 2010; Henry-Bonami et al., 2013). In contrast, very few B cells in the GCs of the 8F10 (0.1%) and V_H125^{SD} (0.3%) mice bound insulin (Fig. 3 B). Quantification of multiple experiments showed that the frequency of the insulin-binding B cells in the GCs of the 8F10-V_H125^{SD} mice was significantly higher than the 8F10 and V_H125^{SD} mice, whereas the GC^- insulin-binding B cells were comparable between the 8F10-V_H125^{SD} and V_H125^{SD} mice (Fig. 3 D). Thus, anti-insulin B cells are specifically selected into GCs from a polyclonal repertoire, where in the presence of 8F10 T helper cells, they underwent a 10–30-fold expansion, correlating with the high titers of IAAs.

Systemic generation of anti-insulin GCs

We next examined such insulin-specific GC formation in other lymphoid organs and found that the mesenteric LNs (mLNs), inguinal (iLNs), and axillary LNs (aLNs) contained 20–50% of insulin-binding B cells (Fig. 4 A, top). The frequency of the insulin-binding B cells in the GCs of the mLN, iLN, and aLN was comparable with pLN (Fig. 4 B). The GCs in the spleen had a moderate number (12%) of insulin-binding B cells (Fig. 4 A, top). In contrast, anti-insulin B cells only constituted a small fraction (≤3%) of the GC^- B cells in all of the lymphoid organs (Fig. 4 A, bottom). Therefore, the development of insulin-specific GCs was systemic, indicating that the very low level of insulin in blood or lymph (Rasio et al., 1967; Yang et al., 1989) must serve as the source of the GC B cell responses.

To evaluate class-switch recombination, we assessed surface IgMa and IgG expression on the GC^+ anti-insulin (GC^+INS^+) B cells as well as the non-GC B cells with high and low insulin-binding mean fluorescence intensities (designated as GC^-INS^{hi} and GC^-INS^{lo}, respectively; gated according to Fig. 4 C). Strikingly, class-switched (IgG^+IgMa^-) B cells (24–45%) were only found in the GC^+INS^+ B cell subset in all the lymphoid sites (Fig. 4 D, top), whereas the GC^-INS^{lo} and GC^-INS^{hi} B cells had very few IgG-bearing B cells (1.1–2.7% and 0.4–1%, respectively), and >80% remained $IgMa^+IgG^-$ (Fig. 4 D, middle and bottom). In addition, many of the IgG-negative GC^+INS^+ B cells (42–59%) had decreased surface IgMa expression ($IgMa^{lo}$), perhaps representing B cells initiating class-switch recombination (Fig. 4 D, top). This IgG^-IgMa^{lo} population was largely absent in the GC^-INS^{lo} (3.1–4.2%) and GC^-INS^{hi} (0.3–1.2%) sub-

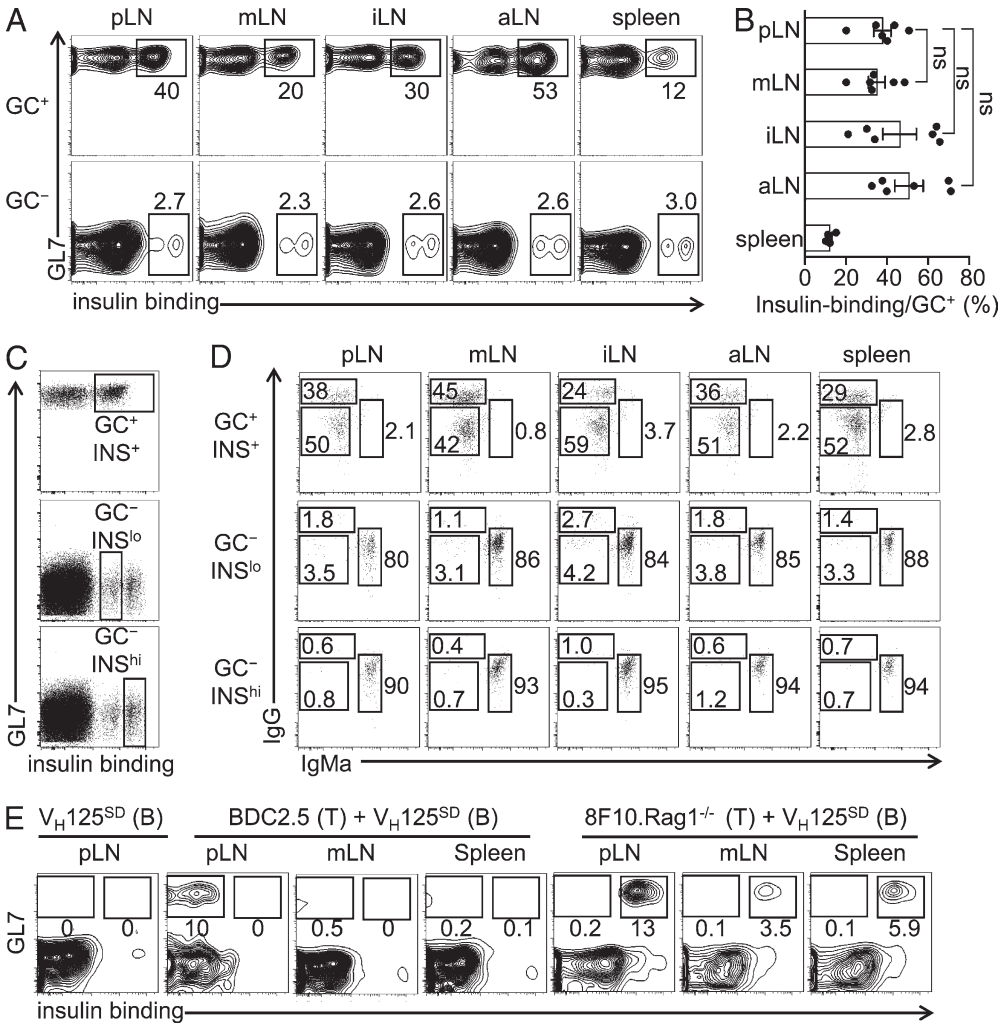

Figure 4. **Anti-insulin GC formation occurs in multiple lymphoid organs.** (A) Insulin binding of the GC^+ and GC^- B cells (gated according to Fig. 3 A) isolated from the pLNs, mLNs, iLNs, and aLNs as well as spleens of the 8F10-V_H125^{SD} mice. (B) Quantification of the frequency of the insulin-binding B cells among GC^+ B cells (mean ± SEM) in multiple sites as assessed in A. ns, not significant; Mann-Whitney test. (C) Gating strategy of the GC^+INS^+, GC^-INS^{lo}, and GC^-INS^{hi} B cells isolated from the 8F10-V_H125^{SD} mice. (D) Surface staining of IgG and IgMa on the GC^+INS^+, GC^-INS^{lo}, and GC^-INS^{hi} B cells from the indicated lymphoid sites of 8F10-V_H125^{SD} mice. (E) GL7 expression and insulin binding on B cells (gated on $CD19^+CD4^-CD8^-$) from NOD.$Rag1^{-/-}$ recipients given FACS-sorted V_H125^{SD} B cells alone or together with naive BDC2.5 or 8F10.$Rag1^{-/-}$ T cells. The NOD.$Rag1^{-/-}$ recipients were killed on day 20 after transfer. Data in A and C–E are representative of three to six independent experiments, and each symbol in B represents one individual experiment.

sets (Fig. 4 D, middle and bottom). Thus, anti-insulin B cells that differentiated into the GC stage are competent to class switch, correlating with the various IgG subclasses of IAAs.

The finding of systemic anti-insulin GC formation was also observed in NOD.$Rag1^{-/-}$ recipients of 8F10.$Rag1^{-/-}$ T cells plus V_H125^{SD} B cells. Specifically, GC responses were found in the pLN, mLN, and spleen of these mice on day 20 after transfer (Fig. 4 E). More importantly, the $GL7^+$ B cells were exclusively insulin specific, further confirming that only anti-insulin B cells can be selected into GCs by the 8F10. $Rag1^{-/-}$ T cells. When naive BDC2.5 T cells were transferred with V_H125^{SD} B cells, they triggered GC reactions only in the pLN, but none of the $GL7^+$ B cells bound insulin (Fig. 4 E). These results confirm that 8F10 T cells directly help insulin-specific B cells to form GCs by using native insulin presented in multiple lymphoid organs.

8F10 T cells differentiate into functional T follicular helper cells (Tfh cells)

Corresponding with the systemic anti-insulin GC responses, development of Tfh cells was found in various LNs of the 8F10-V_H125^{SD} mice (Fig. 5). This was evident by finding CD4 T cells expressing CXCR5 and PD-1, a feature indicating Tfh lineage commitment (Fig. 5 A). RT-PCR analyses revealed that FACS-sorted Tfh cells but not naive T cells expressed genes encoding CXCR5 (*cxcr5*), PD-1 (*pdcd1*), and Bcl-6

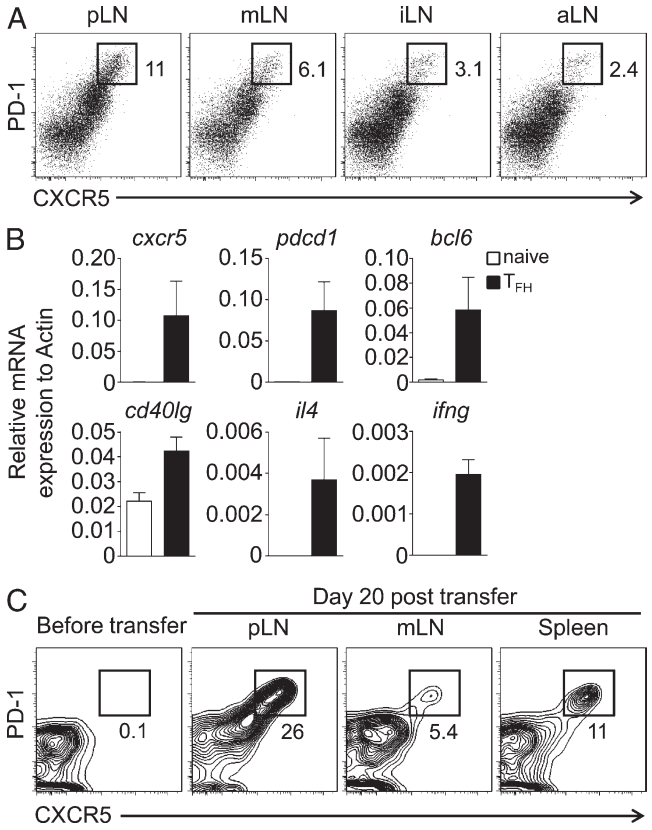

Figure 5. **8F10 T cells differentiate into functional Tfh cells.** (A) FACS plots showing surface CXCR5 and PD-1 staining on $CD4^+CD8^-V\beta8.1/8.2^+CD62L^{lo}$ T cells from LNs of 8F10-V_H125^{SD} mice. (B) RT-PCR analysis of FACS-sorted Tfh ($CD4^+CD8^-B220^-CD25^-CD62L^{lo}CXCR5^{hi}PD\text{-}1^{hi}$) and naive T ($CD4^+CD8^-B220^-CD25^-CD62L^{hi}CD44^-$) cells from pooled LNs of 8F10-V_H125^{SD} mice. (C) FACS-sorted naive 8F10.$Rag1^{-/-}$ T cells were transferred into NOD.$Rag1^{-/-}$ recipients along with V_H125^{SD} B cells. The FACS plots show surface staining of CXCR5 and PD-1 on the naive 8F10.$Rag1^{-/-}$ T cells before transfer and on $CD4^+CD8^-V\beta8.1/8.2^+B220^-$ gated T cells recovered from NOD.$Rag1^{-/-}$ recipients on day 20. Data represent cumulative (B; mean ± SEM) or representative (A and C) results from three independent experiments.

(*bcl6*; Fig. 5 B, top). The Tfh cells also highly expressed genes encoding CD40 ligand (*cd40lg*), IL-4 (*il4*), and IFN-γ (*ifng*; Fig. 5 B, bottom). In the transfer model, naive 8F10.$Rag1^{-/-}$ T cells differentiated into $CXCR5^{hi}PD\text{-}1^{hi}$ Tfh cells in the pLNs, mLNs, and spleen when cotransferred with V_H125^{SD} B cells (Fig. 5 C). Collectively, these results suggest that 8F10 T cells differentiate into committed Tfh cells capable of providing key mediators shaping GC responses and antibody isotypes (Garside et al., 1998; Takahashi et al., 1998; Reinhardt et al., 2009; Crotty, 2011; Victora and Nussenzweig, 2012).

Insulin-specific GC B cells have altered insulin processing and presentation pathways

8F10 T cells specifically recognize the B:12-20 epitope that binds weakly to $I\text{-}A^{g7}$. This peptide segment is edited off when insulin is processed by APCs (Mohan et al., 2011). The findings that 8F10 T cells sustain GC B cell responses and promote conformation-specific antibodies raised a conundrum. It suggested that GC B cells may have altered insulin-processing mechanisms that allow presentation of the 12–20 epitope to 8F10 T cells.

FACS-sorted GC^+INS^+ cells from the 8F10-V_H125^{SD} mice were tested for presentation of insulin epitopes. In parallel, the GC^-INS^{lo} and GC^-INS^{hi} B cells were also sorted and examined. We tested with the 8F10 T cell hybridoma that only recognizes the B:12-20 epitope from pulsing APCs with peptide or denatured insulin but is unreactive to APCs pulsed with insulin (Mohan et al., 2011). The IIT-3 hybridoma specific for the B:13-21 epitope from processing of insulin was tested in parallel (Mohan et al., 2011). Both T cells recognize the B:9-23 peptide that contains both registers.

All of the three B cell subsets pulsed with the B:9-23 peptide robustly stimulated both T cells (Fig. 6 A), indicating their expression of $I\text{-}A^{g7}$ molecules. Each B cell subset pulsed with insulin activated the IIT-3 T cells, indicating that they generated the stronger MHC-binding B:13-21 epitope during insulin processing (Fig. 6 A). Although the GC^-INS^{hi} and GC^-INS^{lo} B cells pulsed with insulin were unable to stimulate the 8F10 T cells, consistent with our previous experiments (Mohan et al., 2010, 2011), the GC^+INS^+ B cells activated 8F10 T cells (Fig. 6 A). Notably, when five times more insulin-pulsed non-GC B cells were used to stimulate 8F10 T cells, a weak response was induced by the GC^-INS^{lo} but not the GC^-INS^{hi} B cells (Fig. 6 B).

The findings that the GC^+INS^+ B cells (gated according to Fig. 6 C) presented the B:12-20 epitope to 8F10 T cells were confirmed in the transfer model (Fig. 6 D). The low recovery of B cells in this model did not permit further fractionation of the GC^-INS^{hi} and GC^-INS^{lo} B cells. Instead, the non–insulin-binding B cells outside GCs (GC^-INS^-) were analyzed (gated according to Fig. 6 C), and this set was unable to activate 8F10 T cells upon insulin pulse (Fig. 6 D).

These results suggest that B cell activation changes the selection of insulin epitopes. To examine this further, we established a cell culture system in which anti-insulin B cells were treated with various stimuli and then tested with the IIT-3 or 8F10 T cell hybridomas for the response to insulin (Fig. 7, A and B). Because of the difficulties in recovering sufficient anti-insulin B cells from the V_H125^{SD} mice, we examined B cells isolated from the 125Tg mice that harbor transgenes expressing the anti-insulin V_H125 and $V_κ125$ chains, giving rise to a monoclonal BCR repertoire in which >98% of B cells were insulin specific (Rojas et al., 2001). Without stimulation, the 125Tg B cells presented insulin to IIT-3 but not 8F10 T cells, indicating that they behaved like unstimulated B cells; that is, capable of presenting the B:13-21 but not the B:12-20 epitope (Fig. 7 A, media). Polyclonal B cells isolated from NOD mice likewise presented insulin to IIT-3 but not to 8F10 T cells (Fig. 7 B, media). The responses in general were considerably weaker

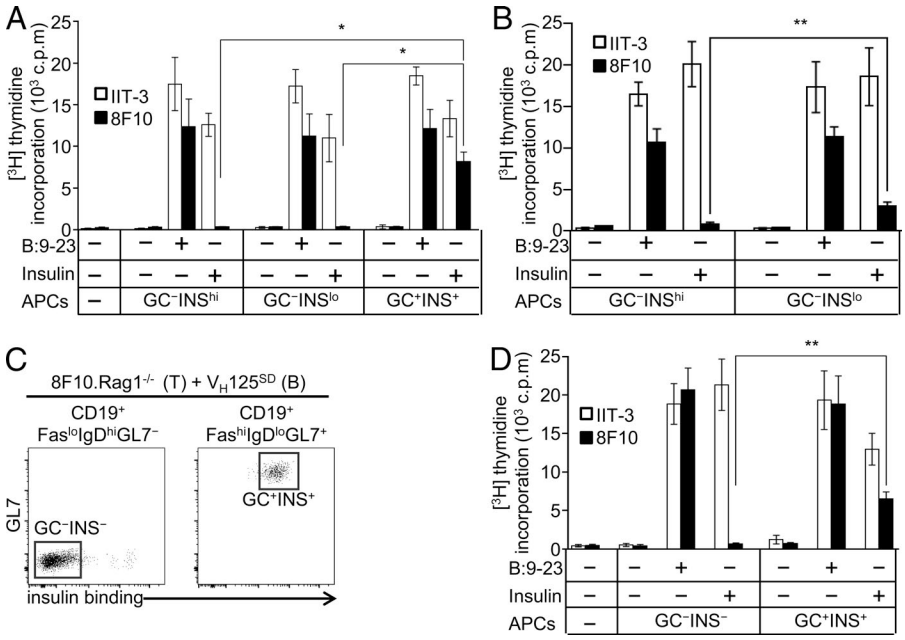

Figure 6. **Insulin-specific GC B cells display an altered pathway for insulin processing and presentation.** (A and B) Response of the IIT-3 and 8F10 T cell hybridomas to the GC^-INS^{hi}, GC^-INS^{lo}, and GC^+INS^+ B cells FACS sorted from the 8F10-V_H125^{SD} mice and pulsed with the B:9-23 peptide or insulin. *, $P < 0.05$; **, $P < 0.05$; paired Student's *t* test. (C) Sorting strategy of the GC^+INS^+ and GC^-INS^- B cells from NOD.$Rag1^{-/-}$ recipients of naive 8F10. $Rag1^{-/-}$ T cells plus V_H125^{SD} B cells on day 20. (D) Response of the IIT-3 and 8F10 T cell hybridomas to the GC^+INS^+ and the GC^-INS^- B cells FACS sorted as in C and pulsed with the B:9-23 peptide or insulin. **, $P < 0.05$; paired Student's *t* test. The B cells (APCs) were used as 2×10^4 per well (A and D) or 10^5 per well (B). Data in A, B, and D represent cumulative results from three independent experiments (mean ± SEM).

than those induced by the 125Tg B cells, signifying a less efficient insulin uptake by WT B cells.

The 125Tg and WT B cells were cultured with the stimuli indicated in Fig. 7 (A and B). 8F10 T cells responded weakly to 125Tg B cells stimulated with soluble CD40 ligand (CD40L) or IL-4 alone, but these two stimuli in combination enabled a strong activation (Fig. 7 A, CD40L + IL-4). Importantly, the cytokine IL-4 was the major molecule ensuring the presentation of the B:12-20 epitope, as indicated by the fact that 125Tg B cells stimulated by LPS combined with IL-4 (LPS + IL-4) but not LPS alone activated 8F10 T cells (Fig. 7 A, bottom). We examined other factors that can

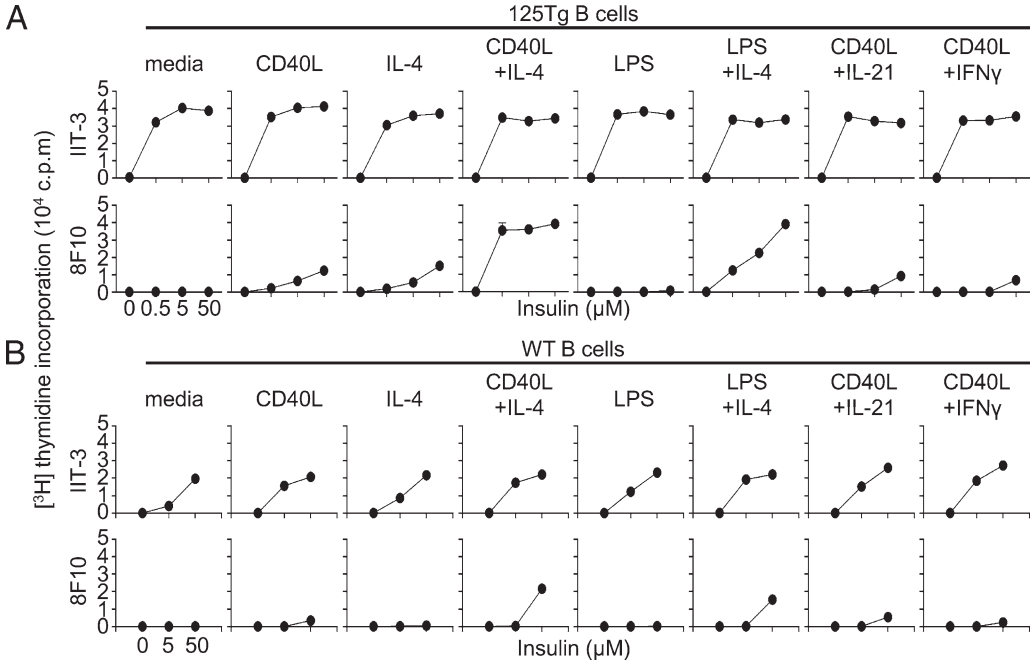

Figure 7. **B cells stimulated by CD40L and IL-4 are able to present the B:12–20 epitope when processing insulin.** (A and B) Response of the IIT-3 and 8F10 T cell hybridomas to 125Tg (A) or WT NOD (B) B cells after stimulation and insulin pulse. The 125Tg and WT NOD B cells were stimulated with the indicated treatments for 18 h and were cultured with serially diluted concentrations of insulin in the presence of the IIT-3 or 8F10 T cell hybridomas. Data are representative of three independent experiments.

be provided by Tfh cells, including the cytokine IL-21 (Linterman et al., 2010; Zotos et al., 2010) and IFN-γ (Reinhardt et al., 2009). Neither of these two cytokines combined with CD40L (CD40L + IL-21 and CD40L + IFN-γ, respectively) further enhanced activation of 8F10 T cells (Fig. 7 A, bottom). Of note, 8F10 T cells responded positively to conventional B cells stimulated by CD40L + IL-4 or LPS + IL-4 at the highest concentration of insulin pulse (Fig. 7 B, bottom). Thus, T cell helper signals, particularly CD40L and IL-4 in synergy, not only function as key mediators regulating GC function but also influence antigen presentation pathways in cognate B cells to ensure optimal and broader T cell–B cell interactions.

DISCUSSION

There are three relevant findings made here that are important for understanding the pathobiology of autoimmune diabetes. First, class-switched IAAs can originate from dynamic interactions between anti-insulin B cells and a unique set of insulin-reactive T cells that recognize the B:12-20 epitope. Second, the native insulin molecule is being presented and recognized by T and B cells in multiple lymphoid sites, indicating that the islet–pLN axis is not the only location capable of fostering insulin autoreactivity. Third, activated B cells, in particular GC B cells, are able to present a broader repertoire of insulin peptides.

Aberrant Tfh cell responses have been associated with autoimmune diseases, including T1D (Vinuesa et al., 2005; Kenefeck et al., 2015; Ueno et al., 2015). In line with this, we found that 8F10 T cells differentiated into Tfh cells and promoted IAA production. These findings revealed a new layer of the functionality of these T cells and largely explained the origin of class-switched IAAs in autoimmune diabetes. In our previous studies, 8F10 T cells escaped thymic selection and were directly recruited into the islets bypassing the pLN (Mohan et al., 2011, 2013). In this study, we observed 8F10 T cell reactivity in peripheral LNs, pointing to recognition of peptide–MHC complexes. It is possible that this recognition is mediated by a subset of resident APCs that can constitutively present the B:12-20 epitope upon insulin processing or by migratory APCs that are activated in the islets or pLN. The B:12-20 epitope may also be available through the presentation of free insulin peptides by all APC subsets expressing MHCII molecules, although whether insulin peptides can be found in the lymph or blood remains to be determined. Dissecting these events may further reveal how naive 8F10 T cells differentiate into effector or Tfh cells in LNs and whether such processes impose pathogenic outcomes. Above all, 8F10 Tfh cells are competent helper cells, as manifested by their expression of Tfh linage markers and T cell help factors. The result that CD40L in combination with IL-4 allowed optimal presentation of the B:12-20 epitope provided a mechanism by which GC B cells interact with 8F10 T cells. Because CD40L and IL-4 also reversed the anergy of anti-insulin B cells (Acevedo-Suárez et al., 2005), our findings propose a model in which signaling events relevant to T cell help, tolerance breakdown, and altered antigen presentation pathways are integrated to ensure anti-insulin GC responses. The mode of action of CD40L plus IL-4, such as regulation of H2-DM and H2-DO expression, is a subject of intense research at present.

The finding of systemic immunoreactivity to insulin indicates that the low concentration (~100 pM) of circulating insulin is sufficient to support GC reactions, even in the spleen, an organ lacking lymphatics. Insulin is also found in lymph (Rasio et al., 1967; Yang et al., 1989) and may enter LNs into the subcapsular sinus to make it available to anti-insulin B cells in the follicles, like other small soluble proteins (Gretz et al., 2000; Pape et al., 2007; Batista and Harwood, 2009; Roozendaal et al., 2009). Therefore, in these instances, spontaneous GC formation may be dependent on persistent availability of a self-antigen rather than on a high concentration. The finding of insulin presentation throughout the lymphoid system should be extrapolated to other endocrine autoimmune diseases in which hormones are the target antigen. The systemic presentation of the hormone could be relevant in two contexts, as in here, where strong CD4 T cell autoreactivity results in B cell activation and autoantibody formation. But also such presentation may be modulatory and may control the activation of both T and B cells (Goodnow et al., 1988; Adelstein et al., 1991; Cooke et al., 1994; Rojas et al., 2001; Acevedo-Suárez et al., 2005; Henry et al., 2009; Zikherman et al., 2012; Kendall et al., 2013).

On the cellular basis, cognate T cell–B cell interactions are required for anti-insulin GC formation. It has been suggested that T cell help is a critical limiting factor for GC selection (Victora et al., 2010) and that GC B cells presenting high amounts of antigens are selectively expanded by Tfh cells (Gitlin et al., 2014). Our results reinforced this notion by showing that the $GC^{+}INS^{+}$ cells actively presented the unconventional B:12-20 epitope, which likely ensured optimal interactions with 8F10 Tfh cells. Beyond efficient antigen presentation by GC B cells (Glazier et al., 2002), our finding further revealed that epitope selection by GC B cells is less constrained, allowing presentation of a broader repertoire of peptides. On the other hand, cellular events concerning how anti-insulin B cells are initially selected into GCs are less understood. We detected a weak presentation of the B:12-20 epitope by the $GC^{-}INS^{lo}$ but not the $GC^{-}INS^{hi}$ B cells. We speculate that this weak response may come from rare B cells making initial contact with 8F10 T cells before the GC phase, an event that may occur at the border of the T cell–B cell zone (Okada and Cyster, 2006). This idea is supported by previous data showing that the $GC^{-}INS^{lo}$ B cells were functionally more activated than the $GC^{-}INS^{hi}$ B cells (Kendall et al., 2007; Henry-Bonami et al., 2013) and that activation of anti-insulin B cells enabled presentation of the B:12-20 epitope.

The cooperativity between anti-insulin T and B cells in exacerbation of diabetes transfer is relevant to the role of B cells in T1D development. Previous studies have shown arrested diabetes progression in the B cell–deficient ($\mu MT^{-/-}$) NOD mice (Serreze et al., 1996; Akashi et al., 1997). In gen-

eral, B cells may contribute to T1D development by functioning as APCs and/or producing anti-islet antibodies. Supporting a role of APCs, impaired effector functions of CD4 and CD8 T cells were observed in $\mu MT^{-/-}$ mice (Greeley et al., 2001; Mariño et al., 2012) and in mice with B cell depletion (Hu et al., 2007). Moreover, ablation of I-A^{g7} in B cells significantly reduced diabetes incidence and insulitis severity (Noorchashm et al., 1999). Given that these manipulations also abolished antibody production, a role of antibody in these models was not excluded. In fact, anti–hen egg lysozyme (HEL) antibodies were able to assist HEL-reactive T cells to trigger diabetes in mice expressing HEL in the islets (Silva et al., 2011). In another study, diabetic autoimmunity was ensured through cooperation between anti-OVA antibodies and OVA-specific CD8 T cells (Harbers et al., 2007). In our model, IAA production is observed concomitantly with exacerbated diabetes development, implying a role of IAAs in assisting T cell responses. Whether IAAs are able to target the islet and directly participate in diabetogenesis through mechanisms involving complement and Fc-γ receptors (Harbers et al., 2007) requires further investigation.

MATERIALS AND METHODS

Mice. NOD/ShiLtJ (NOD), NOD.129S7(B6)-Rag1tm1-Mom/J (NOD.$Rag1^{-/-}$), and NOD.Cg-Tg(TcraBDC2.5, TcrbBDC2.5)1Doi/DoiJ (BDC 2.5) mice were obtained from The Jackson Laboratory.

The 125Tg mice (on the NOD background) expressing anti-insulin BCR heavy and light chain transgenes were described previously (Rojas et al., 2001). The V_H125^{SD} mice that harbor an anti-insulin BCR heavy chain site directed to native IgH locus on the C57BL/6 background (Williams et al., 2015) were backcrossed onto the NOD background for >10 generations. The 8F10 TCR transgenic mice specific for the 12–20 fragment of the insulin B chain (VEALYLVCG; Mohan et al., 2013) were crossed with the V_H125^{SD} mice to generate the 8F10-V_H125^{SD} double transgenic mice. Flow cytometry analyses confirmed that >95% of B cells in the V_H125^{SD} and 8F10-V_H125^{SD} mice were transgenic ($IgMa^+$). The 8F10.$Rag1^{-/-}$ mice were generated by intercrossing the 8F10 mice with the NOD.$Rag1^{-/-}$ mice. All the mice were maintained in specific pathogen-free conditions, and all animal studies were approved by the Division of Comparative Medicine of the Washington University School of Medicine.

Antibodies. The following antibodies were purchased from BioLegend: PerCP-Cy5.5 anti-B220 (RA3-6B2), PE anti-CD103 (2E7), APC-Cy7 anti-CD11c (N418), PE-Cy7 anti-CD4 (RM4-5), BV510 anti-CD45 (30-F11), PerCP-Cy5.5 anti-CD8a (53-6.7), APC anti-F4/80 (BM8), APC anti-CXCR5 (L138D7), Brilliant violet 421 anti-PD1 (29F.1A12), FITC anti-IgMb (AF6-78), PE anti-IgMa (MA-69), and FITC anti-Vβ8.1/8.2 (KJ16-133.18). The following antibodies were purchased from eBioscience: Alexa Fluor 488 anti-GL7 (GL7), PE-Cy7 anti-IgD (11-26), PerCP-eFluor 710 anti-Fas (15A7), PE or eFluor 450 anti-CD19 (1D3), APC anti-CD25 (PC61.5), FITC anti-CD44 (IM7), and PE anti-FoxP3 (FJK-16s). The following antibodies were purchased from BD: PE anti-CD62 ligand (MEL-14), FITC or APC anti-CD3e (145-2C11), and FITC anti-Vβ4 (KT4). APC-conjugated $F(ab')_2$ donkey anti–mouse IgG (H+L) was purchased from Jackson ImmunoResearch Laboratories, Inc., and Pacific blue I-A^{g7} (AG2.42.7) was made in our laboratory.

Flow cytometry and cell sorting. Single-cell suspensions were treated with FcR-blocking media containing 2.4G2 antibodies. The cells were then stained with fluorescent antibodies on ice for 25 min followed by incubation with cell viability dye (eBioscience). For detection of insulin-binding B cells, cells were incubated with 50 ng/ml biotinylated insulin (Eagle Biosciences) with or without inhibition with 500 ng/ml unconjugated insulin for 30 min on ice followed by staining with APC-conjugated streptavidin (BioLegend) for 15 min. The FoxP3 staining was performed using a transcription factor buffer set (eBioscience). The flow cytometry samples were collected using a FACSCanto II (BD), and data were analyzed using FlowJo software (Tree Star). Cell sorting was performed using a FACSAria II (BD).

Islet isolation. The duodenum ampulla was clamped, and the pancreas was perfused with 5-ml calcium-free Hank's balanced salt solution supplemented with 0.4 mg/ml type XI collagenase (Sigma-Aldrich) through the common bile duct. The pancreases were then removed and digested for 15 min at 37°C. After a 90-s shaking, the digestion mixture was washed and passed through a 70-µm cell strainer. The islet-containing fraction retained by the strainer was flushed and stained with 200 mg/ml of the zinc-chelating dye dithizone (Sigma-Aldrich) as a marker of islets. The islets were then handpicked and dispersed in Cell Dissociation Solution Non-Enzymatic (Sigma-Aldrich) for 3 min at 37°C for single-cell suspensions.

Antibody treatment. 4-wk-old female 8F10-V_H125^{SD} mice were injected with anti-CD25 (PC61) antibody or the isotype control Rat IgG i.p. on day 0, 3, 6, and 9 (500 µg per injection). The mice were monitored for diabetes development for another 30 d.

IAA measurement by ELISA. 96-well ELISA plates were coated with 1 µg/well of human insulin (Sigma-Aldrich) overnight at 4°C and were blocked with 3% BSA in PBS. Sera were divided into two equal aliquots that were incubated with or without 10 µg/ml insulin on ice for 1 h. The sera were then added to insulin-coated plates for incubation overnight at 4°C. After extensive washes, the plates were incubated with HRP-conjugated goat anti–mouse IgG1, IgG2a, and IgG2b antibodies (1:10,000; Jackson ImmunoResearch Laboratories, Inc.) for 1 h at room temperature. The enzyme reactions were probed by the OptEIA TMB Substrate Re-

agent Set (BD), and the data were collected using an iMark Microplate Reader (Bio-Rad Laboratories).

B cell stimulation. 125Tg and WT B cells were isolated from spleens by negative selection using magnetic beads (Miltenyi Biotech) with a purity of ≥95%. The cells were plated in V-bottom 96-well plates (10^5 per well) and were cultured with various stimuli, including 500 ng/ml of soluble CD40 ligand (eBioscience), 1 µg/ml LPS (Sigma-Aldrich), and 50 ng/ml recombinant murine IL-4, IL-21, and IFN-γ (PeproTech). After incubation for 18 h, the plates were washed with cold media three times, and the B cells were used for antigen presentation assays.

Antigen presentation assay. FACS-sorted GC and non-GC B cells (2×10^4 per well in Fig. 6 [A and D] and 10^5 per well in Fig. 6 B) were cultured with T cell hybridomas in the presence of 50 µM insulin or 10 µM of the B:9-23 peptide (SHL VEALYLVCGERG). In Fig. 7 (A and B), 125Tg and WT B cells (5×10^4 per well) were cultured with T cell hybridomas in the presence of serially diluted insulin. In all of the assays, T cell hybridomas (5×10^4 per well) were cultured with APCs in round-bottom 96-well plates. After incubation for 18 h, the culture supernatant from each well was collected and used to culture the IL-2–dependent cell line CTLL-2 (10^4 per well). The proliferation of CTLL-2 cells was assessed by [^{3}H]thymidine incorporation.

Adoptive transfer and diabetes monitoring. FACS-sorted naive T cells ($CD4^+CD8^-B220^-CD25^-CD62L^{hi}CD44^-$) from 8F10.Rag1$^{-/-}$ or BDC2.5 mice were transferred i.v. into 4–8-wk-old NOD.Rag1$^{-/-}$ recipients (2×10^5 per mouse). In some experiments, the T cells were cotransferred with 2×10^6 FACS-sorted B cells ($CD19^+CD4^-CD8^-IgMa^+GL7^-IgG^-$) from V_H125^{SD} or WT NOD mice. Blood glucose was monitored daily or weekly (Chemstrip 2GP; Roche), and the mice were considered diabetic with a blood glucose level of ≥250 mg/dl for two consecutive measurements.

RNA isolation and quantitative RT-PCR. Total RNA was isolated from FACS-sorted naive and Tfh cells using the Ambion RNAqueous-Micro kit (Thermo Fisher Scientific) according to the manufacturer's instructions. The cDNA was generated using the iScript Reverse Transcription Supermix (Bio-Rad Laboratories). Quantitative RT-PCR was performed using the PerfeCTa SYBR green Fast Mix (Quanta Biosciences) on a StepOnePlus Real-Time PCR system running StepOne software.

Statistics. The log-rank (Mantel-Cox) test was used to determine significant differences in diabetes incidence. The Mann-Whitney U test was used to determine significant differences between individual biological replicate samples. The paired Student's *t* test was used to calculate p-values of each paired independent experiment with pooled mice.

ACKNOWLEDGMENTS

We thank members of the Unanue laboratory for advice on various aspects of the project. Katherine Fredericks, Rachel Bonami, Kelly Hainz, Chrys Hulbert, and Lindsey Moore helped us on various technical aspects.

Our work was supported by National Institutes of Health grants DK058177, DK020579, AI051448, and R21 DK091692 as well as by the Juvenile Diabetes Research Foundation (SRA-2014-293).

The authors declare no competing financial interests.

Submitted: 29 November 2015
Accepted: 9 March 2016

REFERENCES

Acevedo-Suárez, C.A., C. Hulbert, E.J. Woodward, and J.W. Thomas. 2005. Uncoupling of anergy from developmental arrest in anti-insulin B cells supports the development of autoimmune diabetes. *J. Immunol.* 174:827–833. http://dx.doi.org/10.4049/jimmunol.174.2.827

Achenbach, P., K. Koczwara, A. Knopff, H. Naserke, A.-G. Ziegler, and E. Bonifacio. 2004. Mature high-affinity immune responses to (pro)insulin anticipate the autoimmune cascade that leads to type 1 diabetes. *J. Clin. Invest.* 114:589–597. http://dx.doi.org/10.1172/JCI200421307

Adelstein, S., H. Pritchard-Briscoe, T.A. Anderson, J. Crosbie, G. Gammon, R.H. Loblay, A. Basten, and C.C. Goodnow. 1991. Induction of self-tolerance in T cells but not B cells of transgenic mice expressing little self antigen. *Science.* 251:1223–1225. http://dx.doi.org/10.1126/science.1900950

Akashi, T., S. Nagafuchi, K. Anzai, S. Kondo, D. Kitamura, S. Wakana, J. Ono, M. Kikuchi, Y. Niho, and T. Watanabe. 1997. Direct evidence for the contribution of B cells to the progression of insulitis and the development of diabetes in non-obese diabetic mice. *Int. Immunol.* 9:1159–1164. http://dx.doi.org/10.1093/intimm/9.8.1159

Batista, F.D., and N.E. Harwood. 2009. The who, how and where of antigen presentation to B cells. *Nat. Rev. Immunol.* 9:15–27. http://dx.doi.org/10.1038/nri2454

Bodansky, H.J., P.J. Grant, B.M. Dean, J. McNally, G.F. Bottazzo, M.H. Hambling, and J.K. Wales. 1986. Islet-cell antibodies and insulin autoantibodies in association with common viral infections. *Lancet.* 328:1351–1353. http://dx.doi.org/10.1016/S0140-6736(86)92003-9

Cooke, M.P., A.W. Heath, K.M. Shokat, Y. Zeng, F.D. Finkelman, P.S. Linsley, M. Howard, and C.C. Goodnow. 1994. Immunoglobulin signal transduction guides the specificity of B cell-T cell interactions and is blocked in tolerant self-reactive B cells. *J. Exp. Med.* 179:425–438. http://dx.doi.org/10.1084/jem.179.2.425

Crotty, S. 2011. Follicular helper CD4 T cells (T_{FH}). *Annu. Rev. Immunol.* 29:621–663. http://dx.doi.org/10.1146/annurev-immunol-031210-101400

Dean, B.M., F. Becker, J.M. McNally, A.C. Tarn, G. Schwartz, E.A. Gale, and G.F. Bottazzo. 1986. Insulin autoantibodies in the pre-diabetic period: correlation with islet cell antibodies and development of diabetes. *Diabetologia.* 29:339–342. http://dx.doi.org/10.1007/BF00452073

Ferris, S.T., J.A. Carrero, J.F. Mohan, B. Calderon, K.M. Murphy, and E.R. Unanue. 2014. A minor subset of Batf3-dependent antigen-presenting cells in islets of Langerhans is essential for the development of autoimmune diabetes. *Immunity.* 41:657–669. http://dx.doi.org/10.1016/j.immuni.2014.09.012

Gagnerault, M.-C., J.J. Luan, C. Lotton, and F. Lepault. 2002. Pancreatic lymph nodes are required for priming of β cell reactive T cells in NOD mice. *J. Exp. Med.* 196:369–377. http://dx.doi.org/10.1084/jem.20011353

Garside, P., E. Ingulli, R.R. Merica, J.G. Johnson, R.J. Noelle, and M.K. Jenkins. 1998. Visualization of specific B and T lymphocyte interactions in the lymph node. *Science.* 281:96–99. http://dx.doi.org/10.1126/science.281.5373.96

Gitlin, A.D., Z. Shulman, and M.C. Nussenzweig. 2014. Clonal selection in the germinal centre by regulated proliferation and hypermutation. *Nature.* 509:637–640. http://dx.doi.org/10.1038/nature13300

Glazier, K.S., S.B. Hake, H.M. Tobin, A. Chadburn, E.J. Schattner, and L.K. Denzin. 2002. Germinal center B cells regulate their capability to present antigen by modulation of HLA-DO. *J. Exp. Med.* 195:1063–1069. http://dx.doi.org/10.1084/jem.20012059

Goodnow, C.C., J. Crosbie, S. Adelstein, T.B. Lavoie, S.J. Smith-Gill, R.A. Brink, H. Pritchard-Briscoe, J.S. Wotherspoon, R.H. Loblay, K. Raphael, et al. 1988. Altered immunoglobulin expression and functional silencing of self-reactive B lymphocytes in transgenic mice. *Nature.* 334:676–682. http://dx.doi.org/10.1038/334676a0

Greeley, S.A.W., D.J. Moore, H. Noorchashm, L.E. Noto, S.Y. Rostami, A. Schlachterman, H.K. Song, B. Koeberlein, C.F. Barker, and A. Naji. 2001. Impaired activation of islet-reactive CD4 T cells in pancreatic lymph nodes of B cell-deficient nonobese diabetic mice. *J. Immunol.* 167:4351–4357. http://dx.doi.org/10.4049/jimmunol.167.8.4351

Gretz, J.E., C.C. Norbury, A.O. Anderson, A.E. Proudfoot, and S. Shaw. 2000. Lymph-borne chemokines and other low molecular weight molecules reach high endothelial venules via specialized conduits while a functional barrier limits access to the lymphocyte microenvironments in lymph node cortex. *J. Exp. Med.* 192:1425–1440. http://dx.doi.org/10.1084/jem.192.10.1425

Harbers, S.O., A. Crocker, G. Catalano, V. D'Agati, S. Jung, D.D. Desai, and R. Clynes. 2007. Antibody-enhanced cross-presentation of self antigen breaks T cell tolerance. *J. Clin. Invest.* 117:1361–1369. http://dx.doi.org/10.1172/JCI29470

Henry, R.A., C.A. Acevedo-Suárez, and J.W. Thomas. 2009. Functional silencing is initiated and maintained in immature anti-insulin B cells. *J. Immunol.* 182:3432–3439. http://dx.doi.org/10.4049/jimmunol.0803121

Henry, R.A., P.L. Kendall, E.J. Woodward, C. Hulbert, and J.W. Thomas. 2010. Vkappa polymorphisms in NOD mice are spread throughout the entire immunoglobulin kappa locus and are shared by other autoimmune strains. *Immunogenetics.* 62:507–520. http://dx.doi.org/10.1007/s00251-010-0457-9

Henry-Bonami, R.A., J.M. Williams, A.B. Rachakonda, M. Karamali, P.L. Kendall, and J.W. Thomas. 2013. B lymphocyte "original sin" in the bone marrow enhances islet autoreactivity in type 1 diabetes-prone nonobese diabetic mice. *J. Immunol.* 190:5992–6003. http://dx.doi.org/10.4049/jimmunol.1201359

Höglund, P., J. Mintern, C. Waltzinger, W. Heath, C. Benoist, and D. Mathis. 1999. Initiation of autoimmune diabetes by developmentally regulated presentation of islet cell antigens in the pancreatic lymph nodes. *J. Exp. Med.* 189:331–339. http://dx.doi.org/10.1084/jem.189.2.331

Hoppu, S., M.S. Ronkainen, T. Kimpimäki, S. Simell, S. Korhonen, J. Ilonen, O. Simell, and M. Knip. 2004. Insulin autoantibody isotypes during the prediabetic process in young children with increased genetic risk of type 1 diabetes. *Pediatr. Res.* 55:236–242. http://dx.doi.org/10.1203/01.PDR.0000100905.41131.3F

Hu, C.Y., D. Rodriguez-Pinto, W. Du, A. Ahuja, O. Henegariu, F.S. Wong, M.J. Shlomchik, and L. Wen. 2007. Treatment with CD20-specific antibody prevents and reverses autoimmune diabetes in mice. *J. Clin. Invest.* 117:3857–3867. http://dx.doi.org/10.1172/JCI32405

Hulbert, C., B. Riseili, M. Rojas, and J.W. Thomas. 2001. B cell specificity contributes to the outcome of diabetes in nonobese diabetic mice. *J. Immunol.* 167:5535–5538. http://dx.doi.org/10.4049/jimmunol.167.10.5535

Kendall, P.L., G. Yu, E.J. Woodward, and J.W. Thomas. 2007. Tertiary lymphoid structures in the pancreas promote selection of B lymphocytes in autoimmune diabetes. *J. Immunol.* 178:5643–5651. http://dx.doi.org/10.4049/jimmunol.178.9.5643

Kendall, P.L., J.B. Case, A.M. Sullivan, J.S. Holderness, K.S. Wells, E. Liu, and J.W. Thomas. 2013. Tolerant anti-insulin B cells are effective APCs. *J. Immunol.* 190:2519–2526. http://dx.doi.org/10.4049/jimmunol.1202104

Kenefeck, R., C.J. Wang, T. Kapadi, L. Wardzinski, K. Attridge, L.E. Clough, F. Heuts, A. Kogimtzis, S. Patel, M. Rosenthal, et al. 2015. Follicular helper T cell signature in type 1 diabetes. *J. Clin. Invest.* 125:292–303. http://dx.doi.org/10.1172/JCI76238

Levisetti, M.G., A. Suri, K. Frederick, and E.R. Unanue. 2004. Absence of lymph nodes in NOD mice treated with lymphotoxin-β receptor immunoglobulin protects from diabetes. *Diabetes.* 53:3115–3119. http://dx.doi.org/10.2337/diabetes.53.12.3115

Linterman, M.A., L. Beaton, D. Yu, R.R. Ramiscal, M. Srivastava, J.J. Hogan, N.K. Verma, M.J. Smyth, R.J. Rigby, and C.G. Vinuesa. 2010. IL-21 acts directly on B cells to regulate Bcl-6 expression and germinal center responses. *J. Exp. Med.* 207:353–363. http://dx.doi.org/10.1084/jem.20091738

Mariño, E., B. Tan, L. Binge, C.R. Mackay, and S.T. Grey. 2012. B-cell cross-presentation of autologous antigen precipitates diabetes. *Diabetes.* 61:2893–2905. http://dx.doi.org/10.2337/db12-0006

Mohan, J.F., M.G. Levisetti, B. Calderon, J.W. Herzog, S.J. Petzold, and E.R. Unanue. 2010. Unique autoreactive T cells recognize insulin peptides generated within the islets of Langerhans in autoimmune diabetes. *Nat. Immunol.* 11:350–354. http://dx.doi.org/10.1038/ni.1850

Mohan, J.F., S.J. Petzold, and E.R. Unanue. 2011. Register shifting of an insulin peptide-MHC complex allows diabetogenic T cells to escape thymic deletion. *J. Exp. Med.* 208:2375–2383. http://dx.doi.org/10.1084/jem.20111502

Mohan, J.F., B. Calderon, M.S. Anderson, and E.R. Unanue. 2013. Pathogenic $CD4^+$ T cells recognizing an unstable peptide of insulin are directly recruited into islets bypassing local lymph nodes. *J. Exp. Med.* 210:2403–2414. http://dx.doi.org/10.1084/jem.20130582

Nakayama, M., N. Abiru, H. Moriyama, N. Babaya, E. Liu, D. Miao, L. Yu, D.R. Wegmann, J.C. Hutton, J.F. Elliott, and G.S. Eisenbarth. 2005. Prime role for an insulin epitope in the development of type 1 diabetes in NOD mice. *Nature.* 435:220–223. http://dx.doi.org/10.1038/nature03523

Noorchashm, H., Y.K. Lieu, N. Noorchashm, S.Y. Rostami, S.A.S. Greeley, A. Schlachterman, H.K. Song, L.E. Noto, A.M. Jevnikar, C.F. Barker, and A. Naji. 1999. I-Ag7-mediated antigen presentation by B lymphocytes is critical in overcoming a checkpoint in T cell tolerance to islet β cells of nonobese diabetic mice. *J. Immunol.* 163:743–750.

Okada, T., and J.G. Cyster. 2006. B cell migration and interactions in the early phase of antibody responses. *Curr. Opin. Immunol.* 18:278–285. http://dx.doi.org/10.1016/j.coi.2006.02.005

Pape, K.A., D.M. Catron, A.A. Itano, and M.K. Jenkins. 2007. The humoral immune response is initiated in lymph nodes by B cells that acquire soluble antigen directly in the follicles. *Immunity.* 26:491–502. http://dx.doi.org/10.1016/j.immuni.2007.02.011

Rasio, E.A., C.L. Hampers, J.S. Soeldner, and G.F. Cahill Jr. 1967. Diffusion of glucose, insulin, inulin, and Evans blue protein into thoracic duct lymph of man. *J. Clin. Invest.* 46:903–910. http://dx.doi.org/10.1172/JCI105596

Reinhardt, R.L., H.-E. Liang, and R.M. Locksley. 2009. Cytokine-secreting follicular T cells shape the antibody repertoire. *Nat. Immunol.* 10:385–393. http://dx.doi.org/10.1038/ni.1715

Rojas, M., C. Hulbert, and J.W. Thomas. 2001. Anergy and not clonal ignorance determines the fate of B cells that recognize a physiological autoantigen. *J. Immunol.* 166:3194–3200. http://dx.doi.org/10.4049/jimmunol.166.5.3194

Roozendaal, R., T.R. Mempel, L.A. Pitcher, S.F. Gonzalez, A. Verschoor, R.E. Mebius, U.H. von Andrian, and M.C. Carroll. 2009. Conduits mediate transport of low-molecular-weight antigen to lymph node follicles.

Immunity. 30:264–276. http://dx.doi.org/10.1016/j.immuni.2008.12.014

Serreze, D.V., H.D. Chapman, D.S. Varnum, M.S. Hanson, P.C. Reifsnyder, S.D. Richard, S.A. Fleming, E.H. Leiter, and L.D. Shultz. 1996. B lymphocytes are essential for the initiation of T cell-mediated autoimmune diabetes: analysis of a new "speed congenic" stock of NOD.Ig mu null mice. *J. Exp. Med.* 184:2049–2053. http://dx.doi.org/10.1084/jem.184.5.2049

Silva, D.G., S.R. Daley, J. Hogan, S.K. Lee, C.E. Teh, D.Y. Hu, K.-P. Lam, C.C. Goodnow, and C.G. Vinuesa. 2011. Anti-islet autoantibodies trigger autoimmune diabetes in the presence of an increased frequency of islet-reactive CD4 T cells. *Diabetes.* 60:2102–2111. http://dx.doi.org/10.2337/db10-1344

Takahashi, Y., P.R. Dutta, D.M. Cerasoli, and G. Kelsoe. 1998. In situ studies of the primary immune response to (4-hydroxy-3-nitrophenyl)acetyl. V. Affinity maturation develops in two stages of clonal selection. *J. Exp. Med.* 187:885–895. http://dx.doi.org/10.1084/jem.187.6.885

Ueno, H., J. Banchereau, and C.G. Vinuesa. 2015. Pathophysiology of T follicular helper cells in humans and mice. *Nat. Immunol.* 16:142–152. http://dx.doi.org/10.1038/ni.3054

Unanue, E.R. 2014. Antigen presentation in the autoimmune diabetes of the NOD mouse. *Annu. Rev. Immunol.* 32:579–608. http://dx.doi.org/10.1146/annurev-immunol-032712-095941

Victora, G.D., and M.C. Nussenzweig. 2012. Germinal centers. *Annu. Rev. Immunol.* 30:429–457. http://dx.doi.org/10.1146/annurev-immunol-020711-075032

Victora, G.D., T.A. Schwickert, D.R. Fooksman, A.O. Kamphorst, M. Meyer-Hermann, M.L. Dustin, and M.C. Nussenzweig. 2010. Germinal center dynamics revealed by multiphoton microscopy with a photoactivatable fluorescent reporter. *Cell.* 143:592–605. http://dx.doi.org/10.1016/j.cell.2010.10.032

Vinuesa, C.G., M.C. Cook, C. Angelucci, V. Athanasopoulos, L. Rui, K.M. Hill, D. Yu, H. Domaschenz, B. Whittle, T. Lambe, et al. 2005. A RING-type ubiquitin ligase family member required to repress follicular helper T cells and autoimmunity. *Nature.* 435:452–458. http://dx.doi.org/10.1038/nature03555

Vomund, A.N., B.H. Zinselmeyer, J. Hughes, B. Calderon, C. Valderrama, S.T. Ferris, X. Wan, K. Kanekura, J.A. Carrero, F. Urano, and E.R. Unanue. 2015. Beta cells transfer vesicles containing insulin to phagocytes for presentation to T cells. *Proc. Natl. Acad. Sci. USA.* 112:E5496–E5502. http://dx.doi.org/10.1073/pnas.1515954112

Williams, J.M., R.H. Bonami, C. Hulbert, and J.W. Thomas. 2015. Reversing tolerance in isotype switch-competent anti-insulin B lymphocytes. *J. Immunol.* 195:853–864. http://dx.doi.org/10.4049/jimmunol.1403114

Yang, Y.J., I.D. Hope, M. Ader, and R.N. Bergman. 1989. Insulin transport across capillaries is rate limiting for insulin action in dogs. *J. Clin. Invest.* 84:1620–1628. http://dx.doi.org/10.1172/JCI114339

Zhang, L., and G.S. Eisenbarth. 2011. Prediction and prevention of type 1 diabetes mellitus. *J. Diabetes.* 3:48–57. http://dx.doi.org/10.1111/j.1753-0407.2010.00102.x

Zhang, L., M. Nakayama, and G.S. Eisenbarth. 2008. Insulin as an autoantigen in NOD/human diabetes. *Curr. Opin. Immunol.* 20:111–118. http://dx.doi.org/10.1016/j.coi.2007.11.005

Zikherman, J., R. Parameswaran, and A. Weiss. 2012. Endogenous antigen tunes the responsiveness of naive B cells but not T cells. *Nature.* 489:160–164. http://dx.doi.org/10.1038/nature11311

Zotos, D., J.M. Coquet, Y. Zhang, A. Light, K. D'Costa, A. Kallies, L.M. Corcoran, D.I. Godfrey, K.-M. Toellner, M.J. Smyth, et al. 2010. IL-21 regulates germinal center B cell differentiation and proliferation through a B cell–intrinsic mechanism. *J. Exp. Med.* 207:365–378. http://dx.doi.org/10.1084/jem.20091777